Dalton Transactions

This article can be cited before page numbers have been issued, to do this please use: P. V. Dau, Z. Zhang, P. Dau, J. Gibson and L. Rao, *Dalton Trans.*, 2016, DOI: 10.1039/C6DT01694D.

View Article Online
DOI: 10.1039/C6DT01694D

Journal Name

ARTICLE

Thermodynamic Study of the Complexation between Nd^{3+} and Functionalized Diacetamide Ligands in Solution†

Received 00th January 20xx,
Accepted 00th January 20xx

DOI: 10.1039/x0xx00000x

www.rsc.org/

Phuong V. Dau,[a] Zhicheng Zhang,[a] Phuong D. Dau,[a] John K. Gibson,[a] and Linfeng Rao*[a]

A series of amine functionlized ligands, including 2,2'-(benzylazanediyl)bis(*N,N'*-dimethylacetamide) (BnABDMA), 2,2'-azanediylbis(*N,N'*-dimethylacetamide) (ABDMA), and 2,2'-(methylazanediyl)bis(*N,N'*-dimethylacetamide) (MABDMA), are synthesized for the thermodyamic study of the complexation with Nd^{3+} ions. The complexation in solution is investigated using potentiometry, spectrophotometry, calorimetry, and electrospray ionization mass spectrometry. The results suggest these ligands act as tridentate ligands. Furthermore, direct comparison between ABDMA and an analogous ether-functionalized ligand, 2,2'-oxybis(*N,N'*-dimethylacetamide) (TMDGA), showed that the amine functionalized ligand forms thermodynamically stronger complexes with Nd^{3+} ions than the ether-functionalized ligand. In addition, the amine functionalized ligand can allow the fine-tuning of the binding strength with metal ions via the substitution on the central amine N atom with different functional groups, which is not possible for ether functionalized ligands such as TMDGA.

Introduction

In the past decades, carbon-based fuel energy has been a primary energy source to supply the energy demand of the world. Unfortunately, the use of carbon-based energy relies heavily on the limited coal resources, and has been also criticized for the increase of greenhouse gases in the environment.[1,2] It is thus inevitable to find sustainable, renewable, cleaner, and more efficient energy alternatives to replace current carbon-based fuel energy. Nuclear energy has become a promising alternative resource to replace current carbon-based energy due to its efficacy, reliability and vastly natural uranium ores supply. However, the treatment of nuclear wastes still poses many challenges.[3,4] The high level nuclear waste (HLW) generated during the spent nuclear fuel reprocessing typically contained large quantities of radioactive elements such as U, Pu, Am, Np, Cm, and fission products including lanthanide elements. Efficient separation processes are under development to separate the radioactive elements from the HLW so that the nuclear wastes can be safely disposed of in geological repository. Specifically, the separation between trivalent actinide and lanthanide ions is extremely difficult due to the similarity in their chemical behaviors. Diamide ligands such as the family of alkyl-substituted diglycolamide (TRDGA, Figure 1) ligands[3] have recently become an attractive new class of organic ligands for the application in actinide separation because of their potentials to make the separation process more effective and environmentally benign. In addition, diamide ligands are completely combustible due to their compositions of only C, H, N, and O atoms,[5-26] so that the use of diamide ligands does not increase the volume of solid wastes.

Recently, our group has studied the thermodynamics and solid-state structure of complexes between Nd^{3+} and a ether-functionlized ligand 2,2'-oxybis(*N,N'*-dimethylacetamide) (another name for tetramethyl-diglycolamide, TMDGA, Figure 1).[8] The underlying reason for the study of these ligands is due to their similar structures in comparison with TRDGA ligands such as 2,2'-oxybis(*N,N'*-dioctylacetamide) (another name for tetraoctyl-diglycolamide, TODGA, Figure 1). Thermodynamic and structural studies indicate that the ether-functionalized ligand, TMDGA, coordinates with Nd^{3+} ions in a tridentate mode (the central ether oxygen atom and two amide oxygens atoms) and the complexation was driven by both enthalpy and entropy.[8]

Herein, we report the exploration of a series of amine-functionalized ligands analogous to the ether-functionalized ligand TMDGA previously studied, including 2,2'-(benzylazanediyl)bis(*N,N'*-dimethylacetamide) (BnABDMA), 2,2'-azanediylbis(*N,N'*-dimethylacetamide) (ABDMA), and 2,2'-(methylazanediyl)bis(*N,N'*-dimethylacetamide) (MABDMA, Figure 1) in the complexation with Nd^{3+} ions. The direct comparison between ABDMA and TMDGA can provide an insight of the difference between amine versus ether functionalized ligands in coordinating with Nd^{3+} ions. In addition, the structure of ABDMA allows the substitution with several functional groups such as methyl and benzyl (Figure 1), which cannot be otherwise achieved with the ether-functionalized ligands such as TMDGA. The substitution with different groups modifies the electron density on the central

---

[a] Chemical Science Division, Lawrence Berkeley National Laboratory, One Cyclotron Rd., Berkeley, CA, USA 94720, Email: lrao@lbl.gov, Phone: 1-510-486-5427, Fax: 1-510-486-5596.

†Electronic Supplementary Information (ESI) available: [Titration Conditions, thermograms, and mass spectrophotometry]. See DOI: 10.1039/x0xx00000x

View Article Online
DOI: 10.1039/C6DT01694D

amine N atom so that the binding ability of the ligands can be fine-tuned. The stability constants of the 1:1, 1:2, and 1:3 complexes between these ligands and Nd^{3+} ions were determined via potentiometry and spectrophotometry. Calorimetry was also utilized to experimentally determine the enthalpy of complexation. Furthermore, electrospray ionization mass spectrometry experiments substantiated the formation of these complexes in solution to further support the results from other methods.

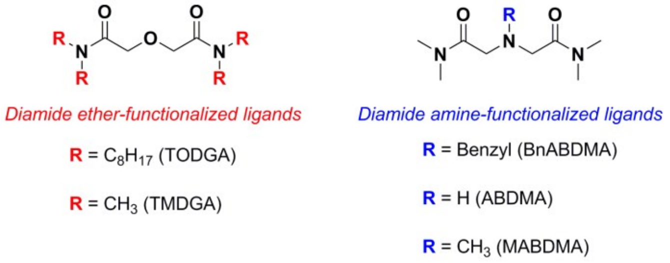

Figure 1. Structures of different ether-functionalized diamide ligands, and amine-functionalized diamide ligands.

Experimental

Starting materials and solvents were purchased and used without further purification from commercial suppliers (Sigma-Aldrich, Alfa Aesar, EMD, TCI, Cambridge Isotope Laboratories, Inc., and others). Proton nuclear magnetic resonance spectra (^1H NMR) were recorded by a Bruker FT-NMR spectrometer (300 MHz). Chemical shifts were quoted in parts per million (ppm) referenced to the appropriate solvent peak or 0 ppm for tetramethylsilane (TMS). The following abbreviations were used to describe the peak patterns when appropriate: br = broad, s = singlet, d = doublet, dd = doublet of doublet, t = triplet, q = quartet, and m = multiplet. Coupling constants, J, were reported in Hertz unit (Hz). Mass spectrophotometry (MS) experiments were performed using an Agilent 6340 quadrupole ion trap mass spectrophotometer.

Milli-Q water was used in preparing all solutions. Nd^{3+} stock solutions were prepared by dissolving $Nd(NO_3)_3{\cdot}xH_2O$ (Aldrich, 99.9%). $NaNO_3$, HNO_3, and NaOH solutions were prepared from solid $NaNO_3$ (Aldrich, 99.9%), concentrated HNO_3 (16 M, Aldrich), and 1 M NaOH (Aldrich). The concentrations of Nd^{3+}, H^+, OH^- in the stock solutions were determined by ethylenediaminetetraacetic acid (EDTA) titrations, Gran's titration,[27] and standard acid/base titration with primary standards (potassium hydrogen phthalate, or tris(hydroxymethyl)aminomethane)), respectively. Ligand solutions were prepared directly by weighting the ligands. The ionic strength of all solutions used in potentiometry, calorimetry, and spectrophotometry was adjusted to 1.0 M at 25 °C by adding appropriate amounts of $NaNO_3$ as the background electrolyte.

In this paper, the neutral ligands, protonated ligands, and the Nd^{3+} complexes are denoted as L, HL^+, and NdL_j^{3+} where j = 1, 2, and 3, respectively.

Ligands Synthesis

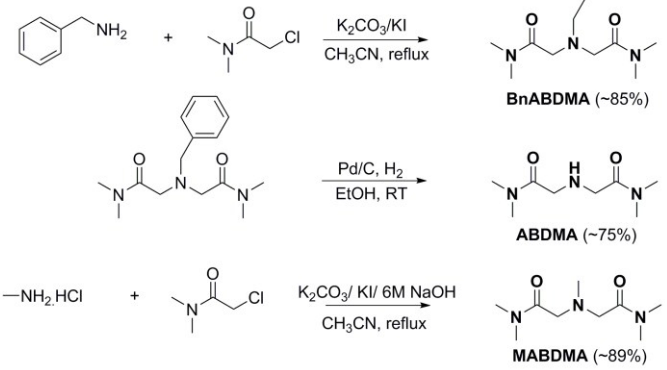

Scheme 1. Synthesis of BnABDMA, ABDMA, and MABDMA.

Synthesis of 2,2'-(benzylazanediyl)bis(N,N'-dimethylacetamide) (BnABDMA, Scheme 1). 2-Chloro-*N,N'*-dimethylacetamide (2.12 mL, 20.50 mmol), benzylamine (1.21 mL, 10.25 mmol), K_2CO_3 (5.50 g, 40.00 mmol), and KI (2.00 g, 12.05 mmol) were added to CH_3CN (~100 mL). The mixture was heated to reflux for 72 h. The mixture was cooled down to room temperature. K_2CO_3 and KI were filtered off. CH_3CN was removed under vacuum conditions to yield a mixture of light yellow liquid and white solid. The mixture was dissolved in $CHCl_3$. Any undissolved solid was then filtered off. $CHCl_3$ was removed under vacuum conditions to yield a light yellow solid as product (2.40 g, 8.71 mmol, ~85%). ^1H NMR ($CDCl_3$, 300 MHz): δ 7.33 (m, 5 H), δ 3.87 (s, 2 H), δ 3.55 (s, 4H), δ 2.94 (s, 6 H), δ 2.90 (s, 6 H). MS ($C_{15}H_{23}N_3O_2$): Calc. [MW] = 277.18, Found $[MW+H]^+$ = 278.2, $[MW+Na]^+$ = 300.2.

Synthesis of 2,2'-azanediylbis(N,N'-dimethylacetamide) (ABDMA, Scheme 1). BnABDMA (1.00 g, 3.60 mmol) was dissolved in ethanol (EtOH, 30 mL) in a scintillation vial. Pd/C (10 wt%, 1.90 g, 1.80 mmol Pd) was added slowly to the scintillation vial. The vial was placed in a Parr bomb reactor. The Parr bomb was sealed and evacuated under vacuum conditions. The bomb reactor was pressurized with H_2 (~5.0 psi). The bomb reactor was evacuated under vacuum conditions and re-pressurized with H_2 (~5.0 psi). The reaction was stirred at room temperature for 3 days. After 3 days, the bomb reactor was evacuated under vacuum conditions and re-pressurized with H_2 (~5.0 psi). The reaction was stirred at room temperature for another 3 days. This process was repeated again. The bomb reactor was then vented. The vial was taken out of the bomb reactor. Pd/C was filtered off with the aid from celite. EtOH was removed under vacuum conditions to yield a white solid as product (383 mg, 2.0 mmol, 57%). ^1H NMR ($CDCl_3$, 300 MHz): δ 3.59 ppm (s, 4H), δ 2.96 ppm (s, 12H), δ 2.17 ppm (br, s, 1H). MS ($C_8H_{17}N_3O_2$): Calc. [MW] = 187.13; Found $[MW+H]^+$ = 188.2 $[MW+Na]^+$ = 210.2.

Synthesis of 2,2'-(methylazanediyl)bis(N,N'-dimethylacetamide) (MABDMA, Scheme 1). 2-Chloro-*N,N'*-dimethylacetamide (2.96 mL, 30.00 mmol), methylamine hydrochloride (1.00 g, 14.80 mmol), K_2CO_3 (6.00 g, ~45 mmol), KI (1.00 g, 6.00 mmol), and 6.0 M NaOH (~1 mL) were added to CH_3CN (~100 mL). The mixture was heat to reflux for 72 h. The mixture was cooled down to room temperature. K_2CO_3 and KI were filtered off. CH_3CN was removed under vacuum conditions to yield a mixture of light yellow liquid and white solid. The mixture was dissolved in $CHCl_3$. Any undissolved solid was then filtered off via vacuum filtration. $CHCl_3$ was removed under vacuum conditions to yield a light yellow sold as product (2.65 g, 13.17 mmol, ~89%). ^{1}H NMR ($CDCl_3$, 300 MHz): δ 3.33 (s, 4 H), δ 2.98 (s, 6H), δ 2.86 (s, 6H), δ 2.36 (s, 3H). MS ($C_9H_{19}N_3O_2$): Calc. [MW] = 201.15, Found $[MW+H]^+$ = 202.2, $[MW+Na]^+$ = 224.2.

Potentiometry

The protonation constants of the ligands and the stability constants of Nd^{3+} complexes with ligands were determined by potentiometric titrations at 25 °C. Titration set up has been reported in detail previously.[8] The titrations were carried out using an automatic titration system consisting of a glass titration cell, a MetroOhm pH meter (model 713), a pH electrode, a MetroOhm dosimat (model 765), and a computer. The temperature of the titration cell was kept at (25 ± 0.1) °C using an external circulating water bath. The titration solutions were kept free of CO_2 via the use of Ar gas. The inner solution of the electrode was replaced with 1M NaCl to reduce the electrode junction potential. Before each titration, the electrode was calibrated using an acid/base titration with standardized HNO_3 and NaOH solutions so that the emf readings could be converted to the concentrations of H^+ in the subsequent titration. For each system, at least 3 independent titrations with different concentrations of ligands, Nd^{3+} ion, or acidity were carried out. The protonation and complexation stability constants were determined by fitting the titration data using the program Hyperquad 2008.[28] The $NdNO_3^{2+}$ complex was included in the fitting model using the stability constant ($\log\beta = -0.19$).[8]

Spectrophotometry

Spectrophotometric titrations were carried out to confirm the stability constants of Nd^{3+} complexes with ligands using a Cary 5G UV-Vis-NIR spectrophotometer with a 10 mm cuvette (1 nm spectral bandwidth). The spectrophotometric titrations were monitored at 620 nm to 560 nm with 0.2 nm step size. For a typical titration experiment, appropriate amount of ligand solution was added into a cuvette containing 2.2 mL of Nd^{3+} solution. The solution in the cuvette was mixed thoroughly for 1-2 minutes before the spectrum was collected. Prior studies have shown that the complexation reaction was fast and the absorbance became stable within 30 seconds of mixing. The stability constants for Nd^{3+} complexes determined by potentiometry were inputted to check the goodness of the fit for the spectrophotometric data via HypSpec.[29] The $NdNO_3^{2+}$ complex was also included in the fitting model using the stability constant ($\log\beta = -0.19$).[8]

Calorimetry

View Article Online
DOI: 10.1039/C6DT01694D

An isothermal microcalorimeter (ITC 4200, Calorimetry Science Corp.) was used to determine the enthalpies of the protonation of ligands and the complexation of Nd^{3+} ion with ligands. Detailed information about this microcalorimeter and the calibration process were reported previously.[8] Multiple titrations using different concentrations of ligands, Nd^{3+}, and H^+ in the initial solution were performed. The enthalpies of protonation and complexation were calculated by analysing the calorimetric data using the HypDeltaH program.[29] The enthalpy of the formation of $NdNO_3^{2+}$, 1.5 kJ mol^{-1},[8] was used as constants in the fitting model.

ESI-Mass Spectrometry

An Agilent 6340 quadrupole ion trap mass spectrometer with a micro electrospray ionization (ESI) source was used to identify Nd^{3+} complexes. Water-ethanol (<5% water) spray solutions were used in the experiments. In high resolution mode, the instrument has a detection range of 50 – 2200 m/z and a resolution of ~0.25 m/z. The intensity distribution of ions in the mass spectra was highly dependent on instrument parameters, which are different when tuning the optimum signals for the tri-cation versus mono-cation complexes. Instrument parameters used to obtain the MS spectra of these complexes were similar to those employed in previous reports.[30,31]

Results and Discussion

Protonation of amine-functionalized ligands

Unlike the ether-functionalized ligands such as TMDGA, the amine functionalized ligands, BnABDMA, ABDMA, and MABDMA, can be protonated in aqueous solution. Figure 2 shows a representative protonation titration of BnABDMA. Representative protonation titrations of ABDMA and MABDMA are shown in Figure S1 of Supporting Information. From multiple titrations, the protonation constants of BnABDMA, ABDMA, and MABDMA ($\log K$, where $K = [HL^+]/([H^+][L])$) are determined to be (6.36 ± 0.03), (7.12 ± 0.03), and (7.64 ± 0.03), respectively, and listed in Table 1. The trend in the protonation constants of the three ligands, BnABDMA < ABDMA < MABDMA, reflects the electron density on the central amine N atom: the electron-withdrawing group such as benzyl makes BnABDMA the more acidic ligand than ABDMA, while the electron-donating methyl group makes MABDMA the more basic ligand than ABDMA.

View Article Online
DOI: 10.1039/C6DT01609D

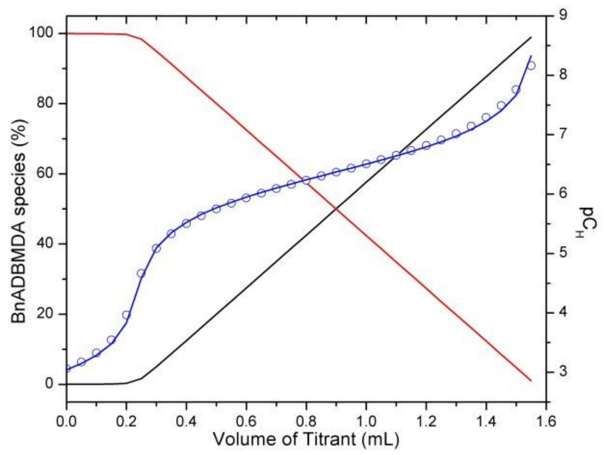

Figure 2. Representative potentiometric titration for the protonation of BnABDMA . I = 1.0 M NaNO$_3$, T = 25 °C. Detailed titration conditions are in Table S1. Symbols: ○ - observed pC$_H$, blue line – calculated pC$_H$; red line – HL$^+$, black line – L.

Stability constants of Nd^{3+} complexes determined by potentiometry

Figure 3 shows representative potentiometric titrations for the complexation of Nd^{3+} ions with the three ligands. Analysis of the experimental data indicates that the data are best described by the formation of three successive Nd^{3+} complexes, as shown by reaction (1):

$$Nd^{3+} + nL = [NdL_n]^{3+} \qquad (1)$$

whereas n = 1, 2, and 3. The stability constants of the 1:1, 1:2, and 1:3 metal to ligand complexes between Nd^{3+} ions and the BnABDMA are (2.92 ± 0.03), (5.08 ± 0.03), and (7.13 ± 0.03), respectively. These stability constants of Nd^{3+} complexes with ABDMA are slightly higher (4.08 ± 0.03, 6.93 ± 0.03, and 10.02 ± 0.03), indicating ABDMA binds stronger to Nd^{3+} ions in comparison to BnABDMA. Similarly, the stability constants of Nd^{3+} complexes with MABDMA are (4.40 ± 0.03), (7.52 ± 0.12), and (12.15 ± 0.03) for the 1:1, 1:2, and 1:3 metal to ligand complexes, respectively. The binding strength of the ligands follow the order: MABDMA > ABDMA > BnABDMA. The stability constants determined by potentiometry are summarized in Table 1.

Stability constants of Nd^{3+} complexes confirmed by spectrophotometry

As shown in Figure 4, the absorption bands of Nd^{3+} are generally red-shifted with additions of ligands, indicating the interactions between the ligands and Nd^{3+} ions.[8] Using the stability constants determined by potentiometry, the spectra were very well fitted for all the complexes except the NdL$_3$$^{3+}$ complex with MABDMA. However, in the case of [Nd(MABDMA)$_3$]$^{3+}$, spectrophotometric titration suggests a much lower stability constant (10.50 ± 0.50) compared to that from the potentiometric data (12.15 ± 0.03). The data from spectrophotometry show that the stepwise stability constants of the Nd^{3+}/MABDMA complexes are 4.40 (NdL^{3+}), 3.12 (NdL$_2$$^{3+}$), and 2.98 (NdL$_3$$^{3+}$), a trend consistent with those for the majority of systems where successive complexes form. In contrast, the potentiometric data show that the *stepwise* stability constants of the Nd^{3+}/MABDMA complexes are 4.40 (NdL^{3+}), 3.12 (NdL$_2$$^{3+}$), and 4.63 (NdL$_3$$^{3+}$). Obviously, the third stepwise stability constant from potentiometry is unreasonable high. We do not have satisfactory explanation for this discrepancy, but the calorimetric data described in a following section indicate that, in the case of Nd(MABDMA)$_3$$^{3+}$, the constant from spectrophotometry (10.50 ± 0.50) provides better fit for the calorimetric titration data.

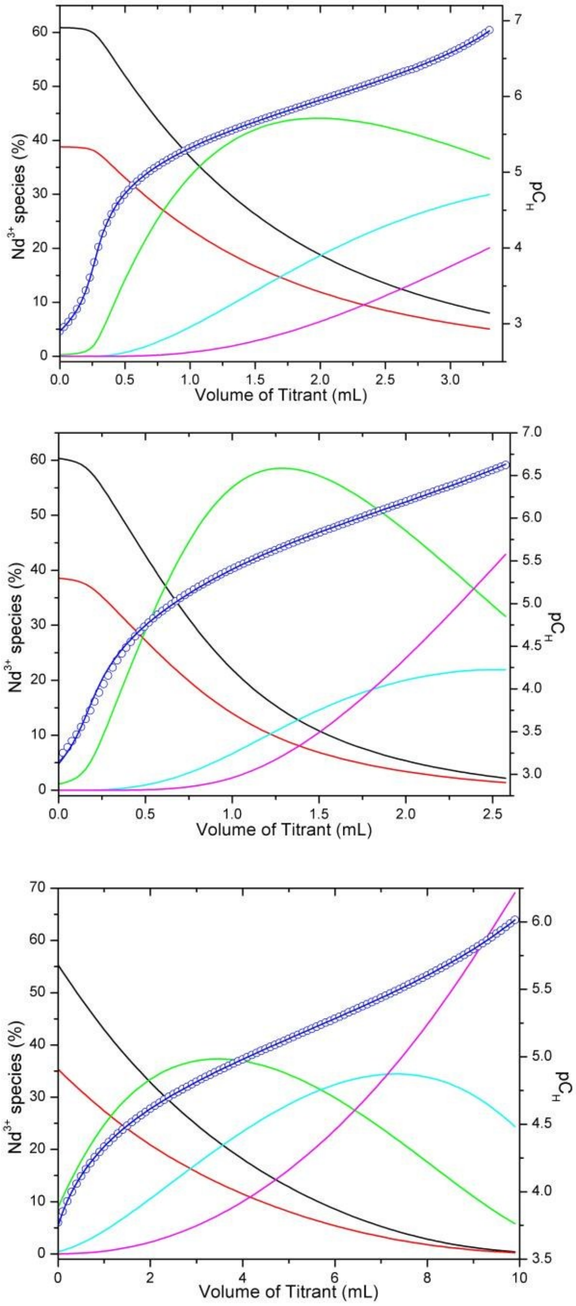

Figure 3. Representative potentiometry titrations and speciation diagrams for the complexation of Nd^{3+} with BnABDMA (top), ABDMA (middle), and MABDMA (bottom) at 25 °C. Detailed titration conditions are in Table S2. Different lines represent Nd^{3+} (black), NdNO$_3$$^{2+}$ (red), NdL^{3+} (green), NdL$_2$$^{3+}$ (cyan), and NdL$_3$$^{3+}$ (magenta). Emptied circle represents observed pC$_H$, and blue line represents the calculated pC$_H$.

View Article Online
DOI: 10.1039/C6DT01694D

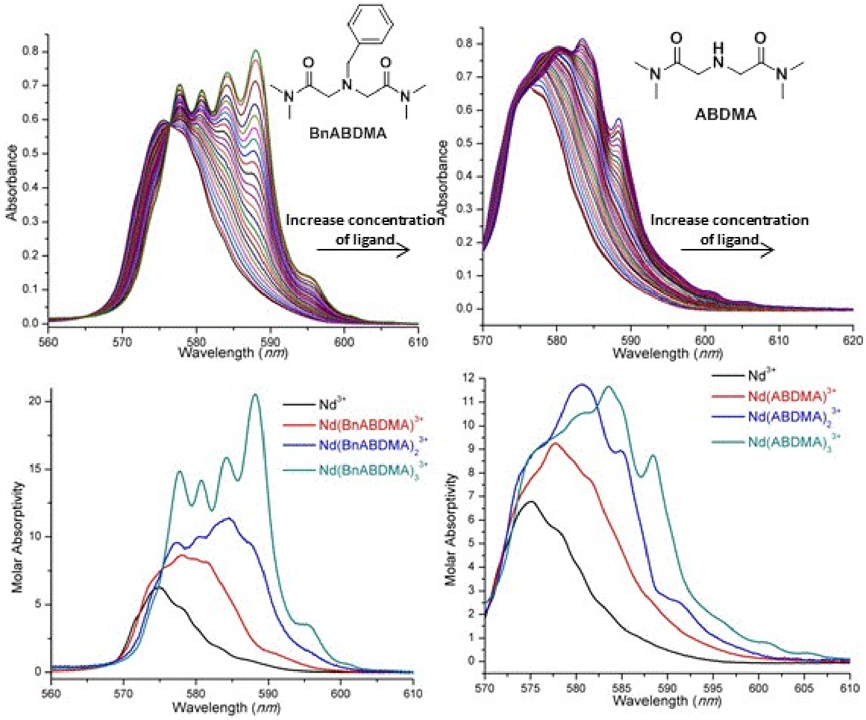

Figure 4. Spectrophotometric titrations of Nd^{3+} complexation with BnABDMA, ABDMA, and MABDMA (top), and molar absorptivity of species (bottom). Detailed titration conditions are in Table S3. The molar absorptivity of $NdNO_3^{2+}$ was omitted for clarity.

Verification the formation of Nd^{3+} complexes by ESI-MS

1:1, 1:2, and 1:3 Nd^{3+}/L complexes for all three ligands were identified by ESI-MS experiments (Figure 5, Figures S4, S5, and S6). The 1:1 and 1:2 Nd^{3+}/L complexes were observed as singly or doubly charged species with NO_3^- as counter anions. In the case of 1:3 Nd^{3+}/L complexes, only a triply charged species is observed. The intensity of the triply charged species is weak but consistent with the natural isotopic abundances of Nd. The weak intensity is due to the lower stability of relatively small complexes with high electric charge, which are susceptible to charge-separation during the ESI process. Since the two spectra in Figure 5 were acquired using different instrumental parameters, the observed results herein cannot be used to quantify the abundance of species,[32] but only to verify the formation of the complexes in a qualitative way. It should be noted that In addition, singly charged NdO^+ specie was also observed in the ESI-MS experiments, potentially due to the reactions between Nd^{3+} and anodic oxidation products of water as reported elsewhere (Figures S4, S5, and S6).[32]

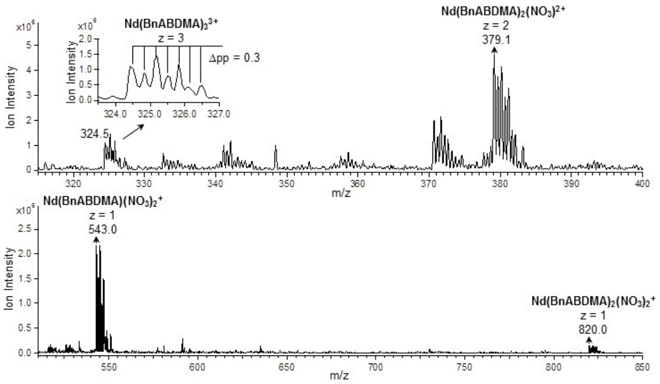

Figure 5. ESI-MS characterization of Nd^{3+} complexes with BnABDMA. In the top spectrum, triply and doubly charged Nd^{3+} complexes were observed, including $Nd(ABDMA)_3^{3+}$ and $Nd(BnABDMA)_2(NO_3)^{2+}$. An inset figure shows a peak to peak separation of Δpp = 0.3 m/z for $Nd(ABDMA)_3^{3+}$. The bottom spectrum shows singly charged complexes of $Nd(BnABDMA)(NO_3)_2^+$ and $Nd(BnABDMA)_2(NO_3)_2^+$.

Enthalpies of protonation of the ligands and enthalpies of Nd^{3+} complexation by calorimetry

At least three independent calorimetric titrations were carried out to determine ΔH of protonation for each ligand (Figure S2).

View Article Online
DOI: 10.1039/C6DT01694D

The values of ΔH of protonation are –(31.20 ± 0.30) kJ mol^{-1}, -(37.2 ± 2.1) kJ mol^{-1}, and –(33.5 ± 0.60) kJ mol^{-1}, for BnABDMA, ABDMA, and MABDMA, respectively. Similarly, multiple titrations were performed in order to determine the ΔH of complexation for the Nd^{3+} complexes. A representative thermalgram of the titration is shown in Figure 6. The experimental heat, calculated heat, and the speciation of Nd^{3+} species in the titrations are shown in Figure 7. The enthalpies of complexation were calculated in conjunction with the stability constants obtained by potentiometry and spectrophotometry. It was found that, in the case of $[Nd(MABDMA)_3]^{3+}$ where significantly different values of stability constants were obtained by potentiometry and spectrophotometry, using the stability constant determined by spectrophotometry allows a better fit than using that determined by potentiometry. Therefore, we elect to designate the value of $\log\beta_3$ = (10.50 ± 0.50) for $[Nd(MABDMA)_3]^{3+}$, and neglect the value of (12.15 ± 0.03) from potentiometry. The enthalpies of protonation and complexation are summarized in Table 1, together with the entropies of complexation accordingly calculated from the enthalpies and stability constants.

Thermodynamic trends in Nd^{3+} complexes with BnABDMA, ABDMA, and MABDMA

Both potentiometric and spectrophotometric experiments indicate that the binding strength of the three ligands follows the trend of the increase in the basicity of the ligands, BnABDMA < ABDMA < MABDMA. This trend can be explained by the electronic effect of the substitution groups in the ligands. In comparison with ABDMA, the electron-withdrawing ability of the phenyl group in BnABDMA reduces the electron density on the central N atom and makes BnABDMA a less basic ligand. Therefore, the Nd^{3+}/BnABDMA complexes are weaker than the Nd^{3+}/ABDMA complexes. On the other hand, the electron-donating ability of the methyl group in MABDMA increases the electron density on the central N atom and makes MABDMA a more basic ligand. Therefore, the Nd^{3+}/MABDMA complexes are stronger than the Nd^{3+}/ABDMA complexes.

The influence of the functional groups on the stability constants implies two aspects of the complexation: (1) the interaction of amine-functionalized ligands with Nd^{3+} is predominantly electrostatic in nature; (2) the central amine nitrogen atoms of these ligands definitely participate in the bonding with the Nd^{3+} ions in solution. It is very likely that, similar to the ether oxygen-functionalized TMDGA, all the three amine-functionalized ligands (BnABDMA, ABDMA, and MABDMA) coordinate to Nd^{3+} ions in a tridentate mode.

Ligand	Method^{a}	Logβ	ΔH (kJ mol^{-1})	ΔS (J K^{-1} mol^{-1})	Ref
TMDGA					8
Nd^{3+} + L = NdL^{3+}	sp, cal	(3.53 ± 0.10)	-(10.9 ± 0.9)	(26 ± 1)	
Nd^{3+} + 2L = NdL_2^{3+}	sp, cal	(5.84 ± 0.19)	-(15.6 ± 1.5)	(39 ± 2)	
Nd^{3+} + 3L = NdL_3^{3+}	sp, cal	(6.80 ± 0.19)	-(19.3 ± 2.2)	(59 ± 7)	
BnABDMA					*this work*
H + L = HL^{+}	pot,cal	(6.36 ± 0.09)	-(31.2 ± 0.3)	(17+1)	
Nd^{3+} + L = NdL^{3+}	pot, sp, cal	(2.92 ± 0.09)	-(13.3 ± 0.6)	(11 ± 1)	
Nd^{3+} + 2L = NdL_2^{3+}	pot, sp, cal	(5.08 ± 0.09)	-(22.6 ± 1.2)	(21 ± 3)	
Nd^{3+} + 3L = NdL_3^{3+}	pot, sp, cal	(7.13 ± 0.09)	-(30.9 ± 0.9)	(33 ± 2)	
ABDMA					*this work*
H + L = HL^{+}	pot, cal	(7.12 ± 0.09)	-(37.2 ± 2.1)	(11+6)	
Nd^{3+} + L = NdL^{3+}	pot, sp, cal	(4.08 ± 0.09)	-(13.5 ± 0.6)	(32± 2)	
Nd^{3+} + 2L = NdL_2^{3+}	pot, sp, cal	(6.93 ± 0.09)	-(20.5 ± 2.1)	(64 ± 6)	
Nd^{3+} + 3L = NdL_3^{3+}	pot, sp, cal	(10.02 ± 0.9)	-(39.4 ± 1.5)	(60 ± 4)	
MABDMA					*this work*
H + L = HL^{+}	pot, cal	(7.64 ± 0.09)	-(33.5 ± 0.6)	(34+2)	
Nd^{3+} + L = NdL^{3+}	pot, sp, cal	(4.40 ± 0.09)	-(11.4 ± 0.3)	(46 ± 1)	
Nd^{3+} + 2L = NdL_2^{3+}	pot, sp, cal	(7.52 ± 0.36)	-(23.4 ± 1.2)	(65 ± 3)	
Nd^{3+} + 3L = NdL_3^{3+}	sp, cal	(10.50 ± 0.50)	-(34.3 ± 1.5)	(86 ± 4)	

Table 1. Overall equilibrium constants, ΔH, and ΔS for the protonation and complexation of BnABDMA, ABDMA, and MABDMA, with Nd^{3+} at 25 °C and I = 1.0 $NaNO_3$. ^{a} Pot: potentiometry, sp: spectrophotometry, cal: calorimetry.

View Article Online
DOI: 10.1039/C6DT01694D

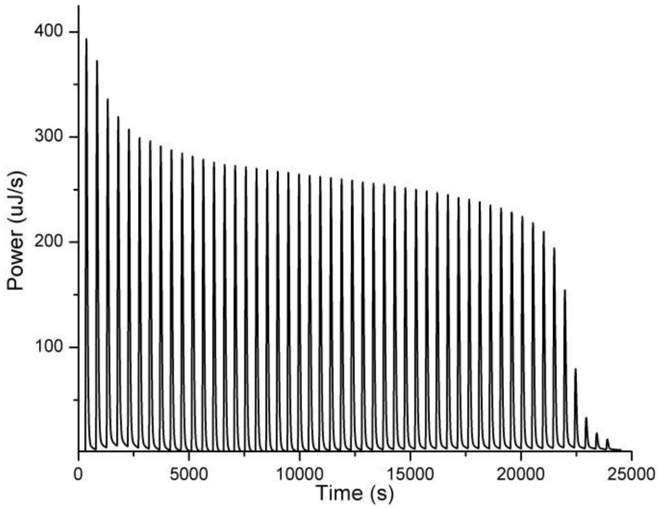

Figure 6. Calorimetric titration thermogram of Nd^{3+} complexation with BnABDMA. V^o = 0.750 mL, injection volume = 0.05 mL, injection interval = 400 s, T = 25 °C. Detailed titration conditions are listed in Table S5.

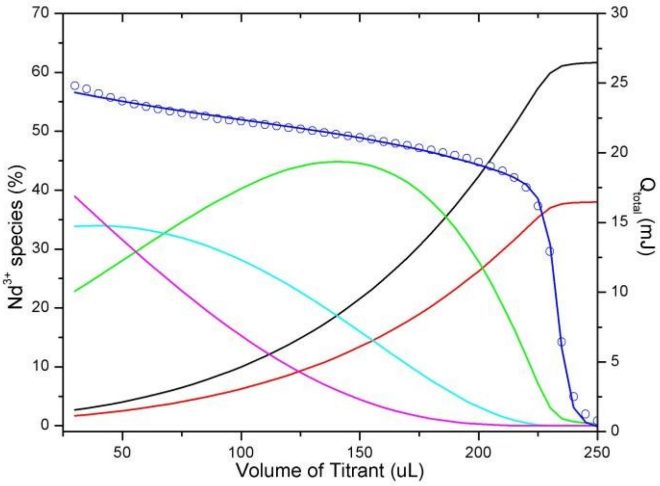

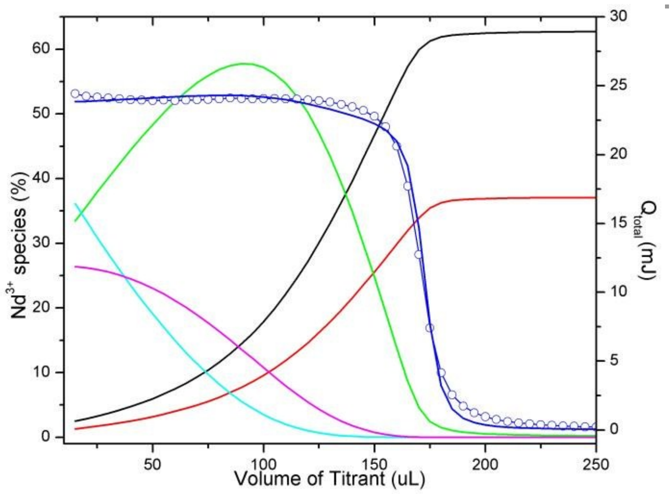

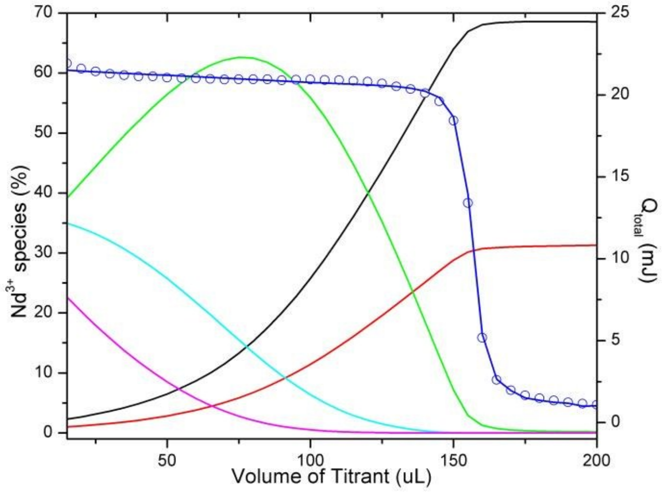

Figure 7. Speciation of Nd^{3+} and heat in calorimetric titrations for Nd^{3+} complexation with BnABDMA (top), ABDMA (middle), and MABDMA (bottom). Detailed titration conditions are in Table S4. Different lines represent Nd^{3+} (black), $(NdNO_3)^{2+}$ (red), $(NdL)^{3+}$ (green), $(NdL_2)^{3+}$ (cyan), and $(NdL_3)^{3+}$ (magenta). Open circle represents observed Q, and blue line represents calculated Q.

Comparison of the binding strength between amine-functionalized ligands and ether oxygen-functionalized TMDGA

In general, the amine-functionalized ligands form stronger complexes with Nd^{3+} than the ether oxygen-functionalized TMDGA (Table 1), except BnABDMA in which the electron-withdrawing phenyl group reduces its binding strength. The higher binding affinity of amine ligands probably results from a combination of a few factors that contribute to the enthalpy of complexation, including the degree of ligand hydration, steric effects and modulation of the nitrogen donor ability by the substitutional groups. This is reflected by the enthalpies of complexation shown in Table 1. The enthalpies of complexation for Nd^{3+} complexes with the amine ligands are generally more exothermic (by a few kilojoules per mole to more than ten kilojoules per mole) than corresponding complexes with TMDGA. It is also interesting to note that the stepwise enthalpies and entropies of complexation (Table S6 in ESI) show different trends for BnABDMA, ABDMA, and MABDMA. Again, the trends reflect the combination of the few effects that contribute to the energetics of the complexation, but it is complicated to assign the origin of these trends to individual effects.

As suggested by the trend in the binding strength of BnABDMA, ABDMA, and MABDMA with Nd^{3+} complexes, the amine nitrogen participates in the coordination with Nd^{3+} and tridentate complexes form. This is similar to the tridentate complexes between Nd^{3+} and TMDGA. However, the binding strength of the amine functionalized ligands can be fine-tuned using different substitutional groups on the central nitrogen atom. Such modification to tune the binding strength is not feasible for the ether-functionalized ligands such as TMDGA or the family of TRDGA ligands.

Conclusions

In summary, thermodynamic parameters of the complexation between Nd^{3+} ions and three amine-functionalized ligands, BnABDMA, ABDMA, and MABDMA, were determined and compared with those of a previously studied ether oxygen-functionalized ligand TMDGA. The binding ability of the amine-functionalized ligands generally form stronger complexes with Nd^{3+} than the ether ligands, due to the difference in the degree of dehydration of the amine nitrogen and the ether oxygen. Besides the higher binding strength, the amine-functionalized ligands offer the advantage of fine-tune the binding strength by using different substitutional groups on the amine nitrogen atom. The trend in thermodynamic parameters within the three amine ligands is consistent with the electronic effect of the substitutional groups on the binding strength.

Acknowledgements

This work was supported by the Director, Office of Science, Office of Basic Energy Science of the U.S. Department of Energy (DOE), under Contract No. DE-AC02-05CH11231 at Lawrence Berkeley National Laboratory (LBNL).

Notes and references

(1) Sumida, K.; Rogow, D. L.; Mason, J. A.; McDonald, T. M.; Bloch, E. D.; Herm, Z. R.; Bae, T.-H.; Long, J. R. *Chem. Rev.* **2012**, *112*, 724.

(2) Suh, M. P.; Park, H. J.; Prasad, T. K.; Lim, D.-W. *Chem. Rev.* **2012**, *112*, 782.

(3) Ansari, S. A.; Pathak, P.; Mohapatra, P. K.; Manchanda, V. K. *Chem. Rev.* **2012**, *112*, 1751.

(4) Panak, P. J.; Geist, A. *Chem. Rev.* **2013**, *113*, 1199.

(5) Tian, G.; Xu, J.; Rao, L. *Angew. Chem. Int. Ed.* **2005**, *44*, 6200.

(6) Tian, G.; Rao, L.; Teat, S. J.; Liu, G. *Chem. Eur. J.* **2009**, *15*, 4172.

(7) Rao, L.; Tian, G.; Teat, S. J. *Dalton Trans.* **2010**, *39*, 3326.

(8) Tian, G.; Teat, S. J.; Rao, L. *Inorg. Chem.* **2014**, *53*, 9477.

(9) Jensen, M. P.; Yaita, T.; Chiarizia, R. *Langmuir* **2007**, *23*, 4765.

(10) Rao, L.; Tian, G. *Mater. Res. Soc. Symp. Proc.* **2006**, *893*, 0893.

(11) Ansari, S. A.; Pathak, P. N.; Husain, M.; Prasad, A. K.; Parmar, V. S.; Manchanda, V. K. *Radiochimica Acta.* **2006**, *94*, 307.

(12) Sasaki, Y.; Choppin, G. R. *Radiochimica Acta.* **1998**, *80*, 85.

(13) Sugo, Y.; Sasaki, Y.; Tachimori, S. *Radiochimica Acta.* **2002**, *90*, 161.

(14) Suzuki, H.; Sasaki, Y.; Sugo, Y.; Apichaibukol, A.; Kimura, T. *Radiochimica Acta.* **2004**, *92*, 463.

(15) Cuillerdier, C.; Musikas, C.; Nigond, L. *Separation Science and Technology* **1993**, *28*, 155.

(16) Horwitz, E. P.; Kalina, D. G.; Kaplan, L.; Mason, G. W.; Diamond, H. *Separation Science and Technology* **1982**, *17*, 1261.

(17) Tian, G.; Zhang, P.; Shen, Y.; Wang, J.; Rao, L. *Separation Science and Technology* **2012**, *47*, 2160.

(18) Gujar, R. B.; Ansari, S. A.; Prabhu, D. R.; Pathak, P. N.; Sengupta, A.; Thulasidas, S. K.; Mohapatra, P. K.; Manchanda, V. K. *Solvent Extraction and Ion Exchange* **2012**, *30*, 156.

(19) Magnusson, D.; Christiansen, B.; Glatz, J.-P.; Malmbeck, R.; Modolo, G.; Serrano-Purroy, D.; Sorel, C. *Solvent Extraction and Ion Exchange* **2009**, *27*, 26.

(20) Murali, M. S.; Mathur, J. N. *Solvent Extraction and Ion Exchange* **2001**, *19*, 61.

(21) Narita, H.; Yaita, T.; Shoichi, T. *Solvent Extraction and Ion Exchange* **2004**, *22*, 135.

(22) Nave, S.; Modolo, G.; Madic, C.; Testard, F. *Solvent Extraction and Ion Exchange* **2004**, *22*, 527.

(23) Sasaki, Y.; Sugo, Y.; Suzuki, S.; Tachimori, S. *Solvent Extraction and Ion Exchange* **2001**, *19*, 91.

(24) Shimada, A.; Yaita, T.; Narita, H.; Tachimori, S.; Okuno, K. *Solvent Extraction and Ion Exchange* **2004**, *22*, 147.

(25) Tian, G.; Wang, J.; Shen, Y.; Rao, L. *Solvent Extraction and Ion Exchange* **2005**, *23*, 519.

(26) Tian, G.; Zhang, P.; Wang, J.; Rao, L. *Solvent Extraction and Ion Exchange* **2005**, *23*, 631.

(27) Gran, G. *Analyst* **1952**, *77*, 661.

(28) Gans, P.; Sabatini, A.; Vacca, A. *Talanta* **1996**, *43*, 1739.

(29) Gans, P.; Sabatini, A.; Vacca, A. *J. Solution Chem.* **2008**, *37*, 467.

(30) Gong, Y.; Hu, H.-S.; Tian, G.; Rao, L.; Li, J.; Gibson, J. K. *Angew. Chem. Int. Ed.* **2013**, *53*, 6885.

(31) Dau, P. D.; Wilson, R. E.; Gibson, J. K. *Inorg. Chem.* **2015**, *54*, 7474.

(32) MacDonald IV, L. W. *Anal. Chem.* **2014**, *86*, 1023.

View Article Online
DOI: 10.1039/C6DT01694D

Three imine-functionalized diamide ligands form tridentate complexes with Nd^{3+} in aqueous solutions. The stability constants of the complexes follow the order of the ligand basicity that can be tuned by different substitutional groups on the imine nitrogen.